Asian Journal of Chemistry; Vol. 24, No. 10 (2012), 4502-4506

ASIAN JOURNAL OF CHEMISTRY

www.asianjournalofchemistry.co.in

Synthesis, Characterization and Photocatalytic Activity of Fe^{3+} Doped Mesoporous TiO_2 Prepared by a Modified Sol-Gel Process

S.Z. HU*, F.Y. LI and Z.P. FAN

Institute of Eco-environmental Sciences, Liaoning Shihua University, Fushun 113001, P.R. China

*Corresponding author: Tel: +86 24 23847473; E-mail: hushaozheng001@163.com

(*Received*: 6 August 2011; *Accepted*: 7 May 2012) AJC-11422

Fe^{3+} doped mesoporous TiO_2 was prepared by a modified sol-gel process. The obtained samples were characterized by X-ray diffraction, N_2 adsorption, FT-IR, UV-VIS spectroscopy and XPS analysis. The prepared TiO_2 samples were around 10-15 nm in size with narrow particle size distribution. The Ti-O-Si bond formed between TiO_2 and MCM-41 fixed the TiO_2 on the MCM-41 surface which restricted the agglomeration and growth of the TiO_2 particles. The performance in photocatalytic degradation of methylene blue under visible light indicated that the addition of MCM-41 greatly improved the photocatalytic activity of prepared TiO_2 catalysts. The doping content of Fe^{3+} and calcination temperature significantly influenced the photocatalytic activity of TiO_2 catalysts.

Key Words: TiO_2, Photocatalysis, MCM-41, Visible light, Fe^{3+}.

INTRODUCTION

TiO_2-based photocatalytic oxidation has received much attention to their application potential for mineralization of many toxic and non-biodegradable organics[1,2]. As a popular photocatalyst, TiO_2 has been widely studied because of its various merits, such as optical-electronic properties, low-cost, chemical stability and non-toxicity[1]. Although TiO_2 has been widely investigated as a photocatalyst in the past decades, its low photo-quantum efficiency and low photocatalytic activity under visible light have limited its usage of solar energy. Therefore, it is highly desirable to develop TiO_2-based photocatalysts with enhanced activities under visible light.

Impurity doping is one of the most useful approaches to resolve those problems. Various metals such as Fe^3, Cr^4, Cu^5, Co^6, Ni^7 and Zn^8 were used to modify TiO_2 catalyst. Among a great variety of metal ion dopants investigated previously, Fe^{3+} is the best candidate due to its suitable band gap energy (*ca.* 2.6 eV) and similar size to that of Ti^{4+} which make it easy to substitute Ti^{4+} into TiO_2 lattice. Generally speaking, the experimental condition, preparation method, target organic compound and standard for the evaluation of photocatalytic activity for each research group are different. Therefore, the effect of metal doping into TiO_2 is controversial[9-12]. Some research groups reported that the Fe^{3+} dopant formed shallow charge traps within the TiO_2 crystal lattice through the substitution of Ti^{4+}, which reduced the electron-hole recombination and improved the photocatalytic efficiency. However, some controversial results which exhibited the detrimental effect for Fe doping have also been reported. Thus, it is not easy to compare those results reported in the previous literatures.

Up to now, many strategies for preparing Fe^{3+} doped TiO_2 have been proposed. Among them, sol-gel method is one of the most widely used. Generally speaking, the TiO_2 prepared by sol-gel process is amorphous which need the calcination procedure to form crystal TiO_2 and then used as photocatalyst. However, high temperature calcination generally gives rise to particle agglomeration and collapse of pore structure, leading to remarkable surface area reduction. The properties mentioned above are significantly important to the photocatalytic performance[2]. To resolve this problem, we report a modified sol-gel method to prepare Fe^{3+} doped mesoporous TiO_2 using MCM-41 as hard template to inhibit the particles aggregation in this paper. A possible mechanism for the photocatalysis was proposed.

EXPERIMENTAL

Preparation and characterization: Siliceous MCM-41 was synthesized following a procedure reported elsewhere[13]. 5 g tetrabutyl titanate and a desired amount of $Fe(NO_3)_3 \cdot 9H_2O$ were dissolved in 12 g ethanol. 2 g MCM-41 was added into above solution under stirring. The formed suspension was stirred to form the gel. The gel was dried at 100 ºC for 2 h and calcined at different temperature for 2 h (heating rate 5 ºC min^{-1}). The obtained solid was added into 30 mL 10 % HF

solution and stirred for 0.5 h to remove the hard template MCM-41. The resulting solid product was washed with deionized water, separated by centrifugation and dried at 50 ºC for 10 h. The obtained TiO_2 powder was denoted as MT(x %)-Y, in which, x % stands for the molar percentage of Fe^{3+} in theoretical product, Y stands for the calcination temperature (ºC). For comparison, two more samples T (1 %)-500 and MT-500 were prepared by the same procedure above but in the absence of MCM-41 and $Fe(NO_3)_3{\cdot}9H_2O$, respectively.

XRD patterns of the prepared TiO_2 samples were recorded on a Rigaku D/max-2400 instrument using CuK_α radiation (λ = 1.54 Å). FT-IR spectra were obtained on a Nicolet 20DXB FT-IR spectrometer. UV-VIS spectroscopy measurement was carried out on a JASCO V-550 model UV-VIS spectrophotometer, using $BaSO_4$ as the reflectance sample. The Brunauer-Emmett-Teller (BET)-specific surface areas (SBET) of the samples were determined through nitrogen adsorption at 77 K (Micromeritics ASAP 2010). All the samples were degassed at 393 K before the measurement. XPS measurements were conducted on a Thermo Escalab 250 XPS system with AlK_α radiation as the exciting source.

Photocatalytic experiment: Methylene blue (MB) was selected as model compound to evaluate the photocatalytic performance of the prepared TiO_2 particles in an aqueous solution under visible light irradiations. 0.1 g of TiO_2 powders were dispersed in 100 mL methylene blue solution (50 ppm) in an ultrasound generator for 10 min. The suspension was transferred into a self-designed glass reactor and stirred for 0.5 h in the dark. For photoreaction under visible light irradiation, the suspension was exposed to a 110-W high-pressure sodium lamp with main emission in the range of 400-800 nm and bubbled with air. The concentrations of methylene blue before and after reaction were measured by means of a UV-VIS spectrophotometer at a wavelength of 665 nm. The percentage of degradation D % was determined as follows:

$$D\,\% = \frac{A_0 - A}{A_0} \times 100\,\% \quad (1)$$

where A_0 and A are the absorbances of the liquid sample before and after degradation, respectively.

RESULTS AND DISCUSSION

Fig. 1 shows the XRD patterns of the obtained TiO_2 particles. The phase contents and the particle sizes of the catalysts were calculated by their XRD patterns according to the method of Spurr[14] and Debye-Scherrer equation[15], respectively. The results shown in Table-1 indicate that the prepared samples were pure anatase TiO_2 except MT(1 %) -700, which anatase/rutile ratio of 3:1. With the same calcination temperature (500 ºC), the particle sizes of Fe doped TiO_2 samples decreased with increasing the doping content. This may be attribute to that the addition of Fe^{3+} occupied regular lattice site of TiO_2 and distorted crystal structure of the host compound due to the different atomic sizes between Fe^{3+} (0.69 Å) and Ti^{4+} (0.745 Å)[16]. With the same doping content (1 %), the particle sizes of Fe doped TiO_2 samples increased with increasing calcination temperature, indicating the particle growth occurred even in the presence of MCM-41 during the calcination procedure. It

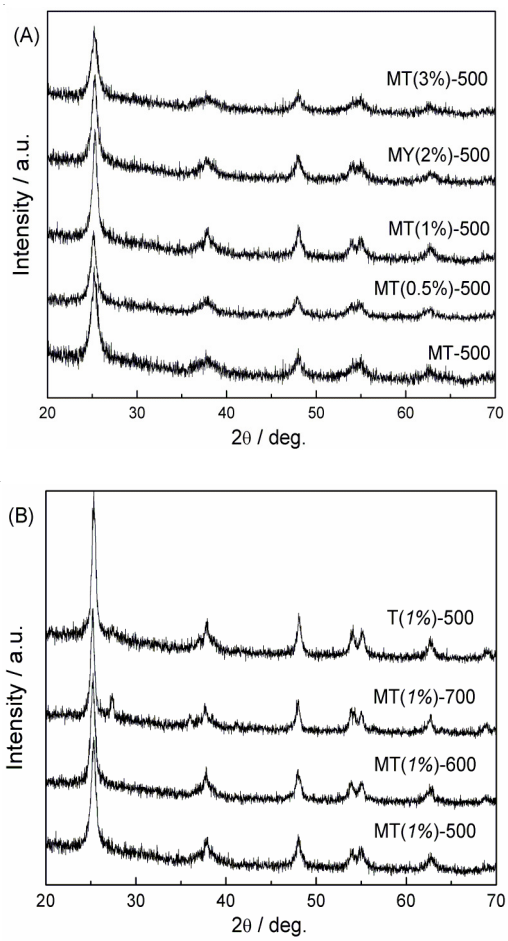

Fig. 1. XRD patterns of prepared samples

is noteworthy that no other crystalline phase containing Fe was observed, even at the highest Fe concentration. This result can likely be explained either by the incorporation of iron(III)-ions in the anatase crystal structure substituting Ti(IV) ions, or by very fine dispersion of Fe_2O_3 in the titania which below the detection limit of this technique.

N_2 adsorption-desorption measurement indicates that mesoporous structure was present for all the Fe^{3+} doped TiO_2 samples prepared in the presence of MCM-41. The N_2 adsorption-desorption isotherm result of MT(1 %)-500 (not shown here) indicated that the isotherm is of classical type IV, suggesting the presence of mesopores in MT(1 %)-500[17]. The BET specific surface area (S_{BET}), pore volume and central pore size are listed in Table-1. The S_{BET} of samples prepared in the presence of MCM-41 were much higher than that of T(1 %)-500. The increased Fe content did not influence S_{BET} of prepared samples with the calcination temperature of 500 ºC. However, the S_{BET} decreased rapidly when increased the calcination temperature. The similar trend was observed for the pore volume (Table-1). These decreased S_{BET} and pore volume might be attributed to the agglomeration among the particles and the pore collapse. The large S_{BET} with mesoporous structure can promote adsorption, desorption and diffusion of reactants and products, which is favorable to the photocatalytic performance.

FT-IR spectra of MT (1 %)-500 before and after HF treatment are shown in Fig. 2. The bands at around 1635 and 3430

TABLE-1
SUMMARY OF PHYSICAL PROPERTIES OF PREPARED TiO_2 SAMPLES

Sample	Size (nm)	X_A/X_R[a] (%)	S_{BET} ($m^2\ g^{-1}$)	Pore volume ($cm^3\ g^{-1}$)	Central pore size (nm)
MT-500	11.5	100 / 0	161	0.42	6.7
MT(0.5 %)-500	11.2	100 / 0	156	0.41	7.1
MT(1 %)-500	11.4	100 / 0	160	0.42	7.2
MT(2 %)-500	10.6	100 / 0	164	0.39	7.6
MT(3 %)-500	9.1	100 / 0	154	0.39	8.2
MT(1 %)-600	13.3	100 / 0	134	0.34	7.8
MT(1 %)-700	15.5	76 / 24	102	0.29	9.2
T(1 %)-500	21	100 / 0	36	0.06	3.4

[a]X_A and X_R represent the phase composition of anatase and rutile, respectively.

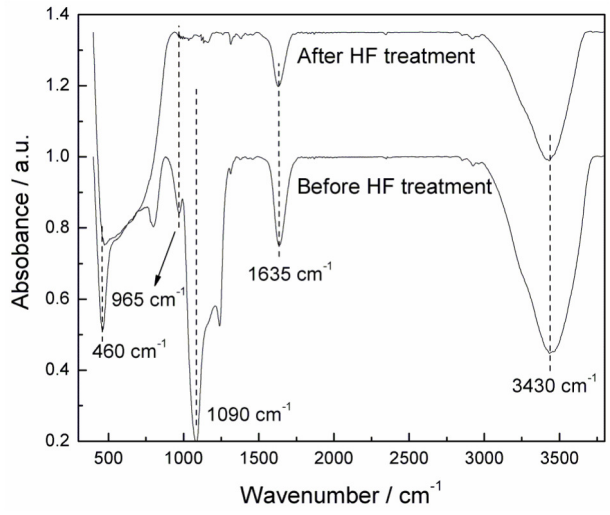

Fig. 2. FT-IR spectra of MT(1 %)-500 before and after HF treatment

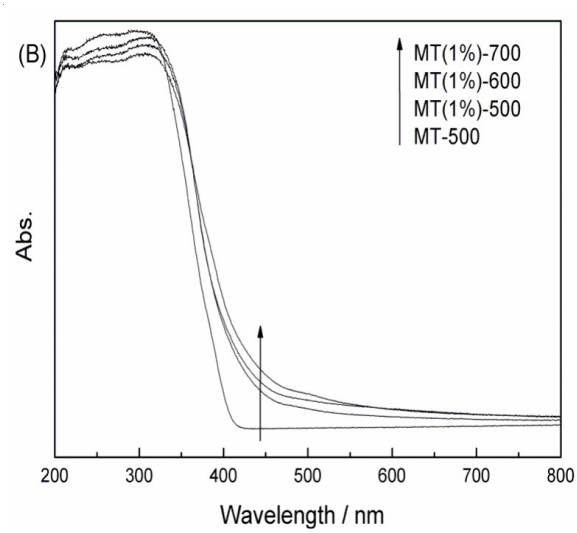

Fig. 3. UV-VIS diffuse reflectance spectra of prepared Fe^{3+} doped TiO_2

cm^{-1} are attributed to the bending and stretching vibrations of hydroxyl groups, respectively. The band at 460 cm^{-1} is attributed to the O-Ti-O structure of TiO_2. In addition, the band at 1090 cm^{-1} which attributed to Si-O-Si structure of MCM-41 disappeared after HF treatment[18]. This hinted that MCM-41 was removed completely by HF treatment. In the spectrum of MT(1 %)-500 before HF treatment, the bands at 965 cm^{-1} was attributed to Ti-O-Si bond formed between TiO_2 and MCM-41[19]. This indicated that not the physical mix but the strong interaction existed between the TiO_2 and MCM-41.

UV-VIS diffuse reflectance spectra of prepared Fe^{3+} doped TiO_2 are shown in Fig. 3. For the neat TiO_2 (MT-500), no absorption in visible region (> 400 nm) was observed. Whereas, Fe^{3+} doped TiO_2 samples exhibited a red shifts of absorption edge and significant enhancement of visible light absorption compared with MT-500. Moreover, the light absorption in the visible range increased with increasing the Fe content (Fig. 4A), accompanied with the changes of colour from white to reddish yellow. Choi *et al.*[20] reported that doping of metal ions in TiO_2 lattice does not change the position of the valence band edge of TiO_2 but introduces new energy level (Fe^{3+}/Fe^{4+}) of the transition metal ions into the band gap of TiO_2. Therefore, the absorption edges shift toward longer wavelengths for the Fe^{3+} doped TiO_2 probably due to the electronic transition from the dopant energy level (Fe^{3+}/Fe^{4+}) to the conduction band of TiO_2.

Fig. 4 shows the XP spectra of MT(1 %)-500 and MT-500 in the region of Ti 2p (A), O 1s (B), Fe 2p (C) and Si 2p (D). Compared with the spectra of MT-500, slight shifts to

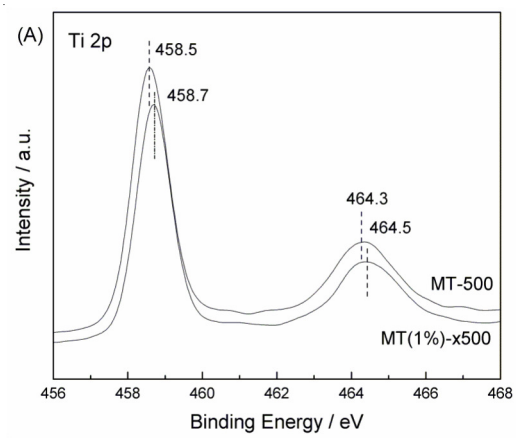

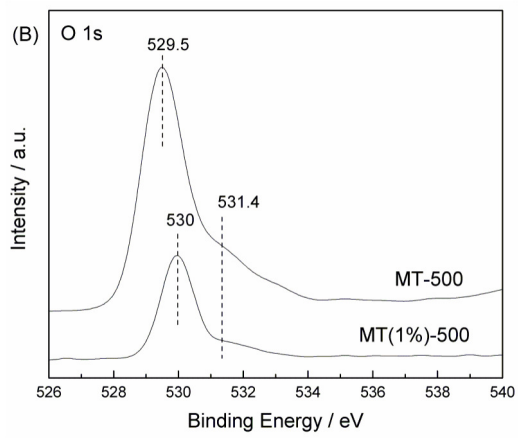

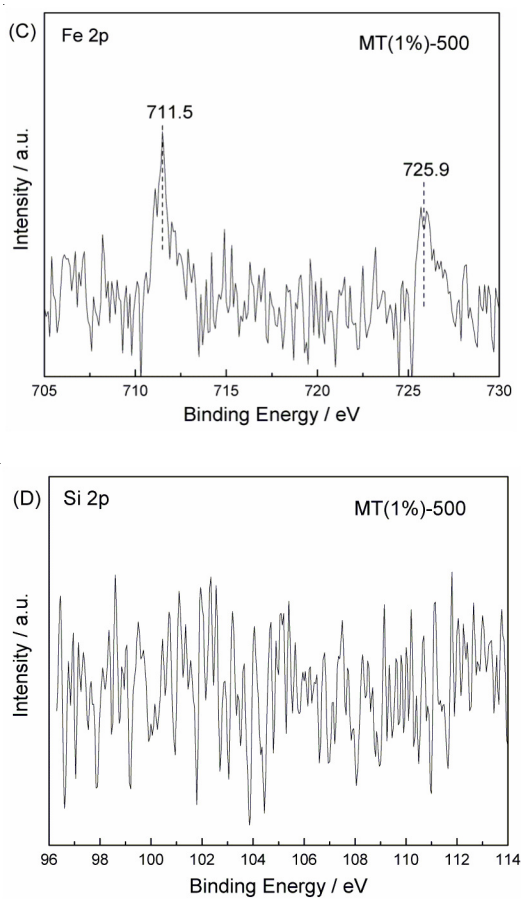

Fig. 4. XP spectra of MT(1 %)-500 and MT-500 in the region of Ti 2p (A), O 1s (B), Fe 2p (C) and Si 2p (D)

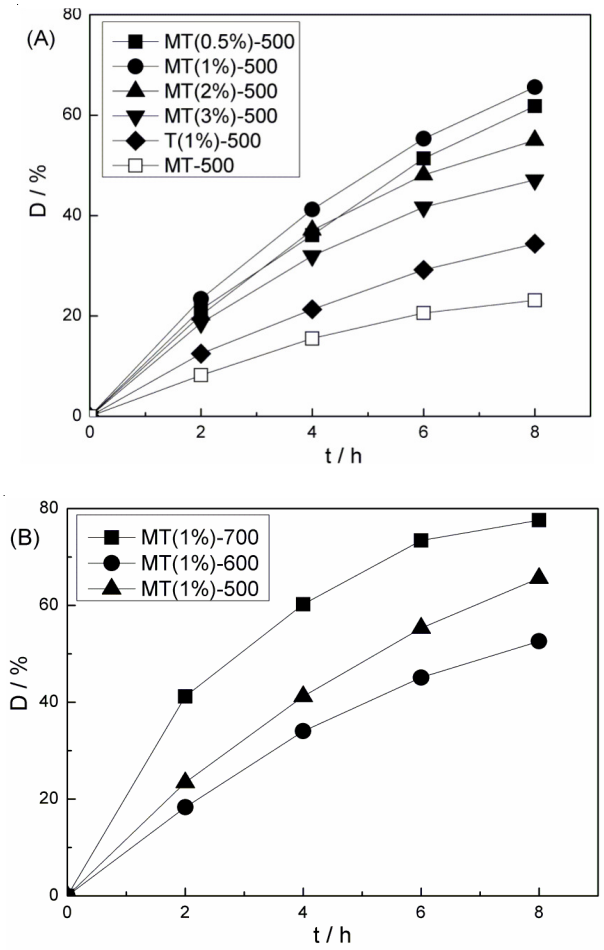

Fig. 5. Percentage degradation of methylene blue in aqueous solution under visible light as a function of reaction time

higher binding energies were observed for MT (1 %)-500 in the Ti 2p region (458.7 and 464.5 eV) as well as the O 1s region (530 eV). Yalçin *et al.*[21] considered that the Fe^{3+} was doped into TiO_2 lattice to form Ti-O-Fe bond which caused the change of chemical environment, thus led to the binding energy shifts. In Fig. 4C, the binding energies around 711.5 and 725.9 eV should be assigned to $2p_{3/2}$ and $2p_{1/2}$ of Fe^{3+}, respectively. These data exhibit obvious shift to higher binding energy compared to those in Fe_2O_3 (710.7 and 724.3 eV for $2p_{3/2}$ and $2p_{1/2}$)[22]. This result farther proved that Fe^{3+} was not existed as oxide but replaced Ti^{4+} to form Ti-O-Fe bond. The binding energy of Si 2p in SiO_2 is around 103-104 eV[23]. However, no peak was observed in Fig. 4D indicated the MCM-41 was removed completely after HF treatment.

The photocatalytic activities of prepared TiO_2 catalysts were tested by the degradation of MB under visible light and the results were shown in Fig. 5. All the Fe^{3+} doped TiO_2 catalysts showed much higher photocatalytic activities than that of neat TiO_2 MT-500 (Fig. 5A). The enhanced photocatalytic activities must result from the doping of Fe^{3+} in TiO_2, which gave rise to the narrowed band gap and thus to the enhanced absorption in the visible region. The t_{2g} level of 3d orbital of Fe^{3+} ion is above the valence band of TiO_2[22]. Therefore, Fe^{3+} ion can absorb a photon with wavelength exceeding 400 nm to produce a Fe^{4+} ion and a TiO_2 conduction band electron (eqn. 2). Due to the energy level for Fe^{3+}/Fe^{2+} is below the conduction band edge of TiO_2[24], Fe^{3+} ions can trap this conduction band electron and turn into Fe^{2+} (eqn. 3). According to the viewpoint of crystal field theory[3], Fe^{2+} and Fe^{4+} ions are relatively unstable compared with Fe^{3+} ions, which have half-filled $3d^5$ orbital. Therefore, the Fe^{2+} and Fe^{4+} ions can easily release the electrons and holes respectively and turn back to Fe^{3+}. The released electrons and holes migrate to the surface of TiO_2 to initiate the photocatalytic reaction. Fe^{2+} ions can be oxided to Fe^{3+} ions by transferring electrons to O_2 absorbed on TiO_2 surface (eqn. 4) or a neighboring surface Ti^{4+} ions (eqn. 5). The adsorbed O_2 is reduced to O_2^- (eqns. 4 and 6), which is responsible for the degradation of methylene blue. Similarly, Fe^{4+} ions are reduced to Fe^{3+} ions by releasing holes (eqn. 7). The released holes react with OH^- to generate $^{\cdot}OH$, which is another active oxygen species to degrade the methylene blue.

$$Fe^{3+} + h\nu \rightarrow Fe^{4+} + e^- \quad (2)$$

$$Fe^{3+} + e^- \rightarrow Fe^{2+} \quad (3)$$

$$Fe^{2+} + O_2(ads) \rightarrow Fe^{3+} + O_2^- \quad (4)$$

$$Fe^{2+} + Ti^{4+} \rightarrow Fe^{3+} + Ti^{3+} \quad (5)$$

$$Ti^{3+} + O_2(ads) \rightarrow Ti^{4+} + O_2^- \quad (6)$$

$$Fe^{4+} + OH^-(ads) \rightarrow Fe^{3+} + OH^{\bullet}(ads) \quad (7)$$

In Fig. 5A, the photocatalytic activities of Fe^{3+} doped TiO_2 increased with increasing Fe^{3+} content and then has a downtrend when the Fe^{3+} content beyond 1 %. This is due to that Fe^{3+} could act as the recombination center for the

photogenerated electron and hole, according to the reactions of eqns. 3 and 8-11. When the dopant concentration is too high, the recombination rate will increase and compete with the redox processes because the distance between trapping sites decreases[25]. Moreover, in the presence of MCM-41, the obtained catalysts (MT(x %)-500) exhibited much higher photocatalytic activities than that of T(1 %) -500. These increased activities may be attributed to the smaller particle sizes of MT(x %)-500 compared with T(1 %)-500. The number of surface active sites may increase with the decrease in the particle size, leading to the increase in the surface charge carrier transfer rate in photo-catalysis process and thus the decrease in the electron-hole recombination. Moreover, the addition of MCM-41 caused the SBET of prepared Fe^{3+} doped TiO_2 much higher than that of T(1 %)-500 (Table-1). The higher surface area may facilitate the adsorption of hydroxyl groups, which trap the photo-generated to produce active surface hydroxyl radicals. These hydroxyl radicals play crucial roles in photo-catalytic reactions[26].

$$Fe^{3+} + h^+ \rightarrow Fe^{4+} \quad (8)$$

$$Fe^{2+} + h^+ \rightarrow Fe^{3+} \quad (9)$$

$$Fe^{4+} + e^- \rightarrow Fe^{3+} \quad (10)$$

$$Fe^{2+} + OH^{\bullet} \rightarrow Fe^{3+} + OH^- \quad (11)$$

In Fig. 5B, MT(1 %)-500 exhibited higher photocatalytic activity than MT(1 %)-600. This maybe due to the smaller particle size of MT(1 %)-500 compared with MT(1 %)-600. Moreover, it is interesting that MT(1 %)-700 showed the highest photocatalytic activity among the three catalysts although its particle size is the biggest. This maybe attribute to the synergetic effect between the anatase and rutile phase of MT(1 %)-700. The band gap of anatase and rutile TiO_2 is 3.2 and 3.0 eV, respectively. The conduction band of rutile was considered to be at a lower level than that of anatase. The coupling of two phases allowed the migration of photogenerated electrons from anatase phase to rutile phase and retarded the recombination of the electrons and holes in anatase[27]. On the other hand, the UV-VIS result showed that MT(1 %)-700 absorbed more visible light compared with others. Therefore, it is reasonable that MT(1 %)-700 exhibited the highest photocatalytic activity under visible light.

Conclusion

Fe^{3+} doped mesoporous TiO_2 was prepared by a modified sol-gel process. The prepared TiO_2 samples were around 10-15 nm in size with narrow particle size distribution. The Ti-O-Si bond formed between TiO_2 and MCM-41 fixed the TiO_2 on MCM-41 surface which restricted the agglomeration and growth of the TiO_2 particles. Distinct shifts of the absorption bands into the visible light region were observed for prepared Fe^{3+} doped TiO_2. Fe^{3+} was doped by replacing the Ti^{4+} in TiO_2 lattice which introduced the new energy level (Fe^{3+}/Fe^{4+}) into the band gap. The addition of MCM-41 greatly improved the photocatalytic activity of prepared Fe^{3+} doped TiO_2 catalysts under visible light. The optimal doping content is 1 %. MT(1 %)-700 exhibited the highest photocatalytic activity among the prepared catalysts which attributed to the synergetic effects of Fe^{3+}-doping, large SBET, small particle size and mix crystal effect.

ACKNOWLEDGEMENTS

This work was supported by National Natural Science Foundation of China (No. 41071317, 30972418), National Key Technology R & D Programme of China (No. 2007BAC16B07), the Natural Science Foundation of Liaoning Province (No. 20092080). The authors would like to thank Prof. Anjie Wang, Dalian University of Technology, for the contribution to the manuscript.

REFERENCES

1. A. Fujishima, T.N. Rao and D.A. Tryk, *J. Photochem. Photobiol. C*, **1**, 1 (2000).
2. M.R. Hoffmann, S.T. Martin, W. Choi and D.W. Bahnemann, *Chem. Rev*., **95**, 69 (1995).
3. M.H. Zhou, J.G. Yu and B. Cheng, *J. Hazard. Mater*., **137**, 1838 (2006).
4. H. Irie, T. Shibanuma, K. Kamiya, S. Miura, T. Yokoyama and K. Hashimoto, *Appl. Catal. B*, **96**, 142 (2010).
5. S. Yamazaki, M. Sugihara, E. Yasunaga, T. Shimooka and K. Adachi, *J. Photochem. Photobiol. A*, **209**, 74 (2010).
6. J. Wang, Y.H. Lv, Z.H. Zhang, Y.Q. Deng, L.Q. Zhang and B. Liu, *J. Hazard. Mater*., **170**, 398 (2009).
7. H. Yu, X.J. Li, S.J. Zheng and W. Xu, *Mater. Chem. Phys*., **97**, 59 (2006).
8. W.J. Zhang, S.L. Zhu, Y. Li and F.H. Wang, *Vacuum*, **82**, 328 (2008).
9. H. Yamashita, M. Harada, J. Misaka, M. Takeuchi, B. Neppolian and M. Anpo, *Catal. Today*, **84**, 191 (2003).
10. X.Y. Li, P. Yue and C. Kutal, *New J. Chem*., **27**, 1264 (2003).
11. K. Nagaveni, M.S. Hegde and G. Madras, *J. Phys. Chem. B*, **108**, 20204 (2004).
12. E.P. Reddy, B. Sun and P.G. Smirniotis, *J. Phys. Chem. B*, **108**, 17198 (2004).
13. A. Wang and T. Kabe, *Chem. Commun*., 2067 (1999).
14. R.A. Spurr and H. Myers, *Anal. Chem*., **29**, 760 (1957).
15. J. Lin, Y. Lin, P. Liu, M.J. Meziani, L.F. Allard and Y.P. Sun, *J. Am. Chem. Soc*., **124**, 11514 (2002).
16. Z.J. Li, W.Z. Shen, W.S. He and X.T. Zu, *J. Hazard. Mater*., **155**, 590 (2008).
17. K.S.W. Sing, D.H. Everett, R.A.W. Haul, L. Moscou, R.A. Pierotti and J. Rouquerol, *Pure Appl. Chem*., **57**, 603 (1985).
18. K.Y. Jung and S.B. Park, *Appl. Catal. B*, **25**, 249 (2000).
19. D.W. Lee, S.K. Ihm and K.H. Lee, *Chem. Mater*., **17**, 4461 (2005).
20. W. Choi, A. Termin and M.R. Hoffmann, *J. Phys. Chem*., **98**, 13669 (1994).
21. Y. Yalçin, M. Kiliç and Z. Çinar, *Appl. Catal. B*, **99**, 469 (2010).
22. J.F. Zhu, F. Chen, J.L. Zhang, H.J. Chen and M. Anpo, *J. Photochem. Photobiol. A*, **180**, 196 (2006).
23. D. Dudeck, A. Yanguas-Gil, F. Yubero, J. Cotrino, J.P. Espinós and W. Cruz, *Surf. Sci*., **601**, 2223 (2007).
24. Y. Ma, X.T. Zhang, Z.S. Guan, Y.A. Cao and J.N. Yao, *J. Mater. Res*., **16**, 2928 (2001).
25. F.B. Li, X.Z. Li, M.F. Hou, K.W. Cheah and W.C.H. Choy, *Appl. Catal. A*, **285**, 181 (2005).
26. S.Z. Hu, A.J. Wang, X. Li, Y. Wang and H. Löwe, *Chem. Asian J*., **5**, 1171 (2010).
27. J.G. Yu, J.F. Xiong, B. Cheng and S.W. Liu, *Appl. Catal. B*, **60**, 211 (2005).